International Journal of Mechanical, Industrial and Aerospace Sciences
ISSN: 2517-9950
Vol:5, No:3, 2011

Application of Fuzzy Logic Approach for an Aircraft Model with and without Winglet

Altab Hossain, Ataur Rahman, Jakir Hossen, A.K.M. P. Iqbal, and SK. Hasan

***Abstract*—**The measurement of aerodynamic forces and moments acting on an aircraft model is important for the development of wind tunnel measurement technology to predict the performance of the full scale vehicle. The potentials of an aircraft model with and without winglet and aerodynamic characteristics with NACA wing No. 65-3-218 have been studied using subsonic wind tunnel of 1 m × 1 m rectangular test section and 2.5 m long of Aerodynamics Laboratory Faculty of Engineering (University Putra Malaysia). Focusing on analyzing the aerodynamic characteristics of the aircraft model, two main issues are studied in this paper. First, a six component wind tunnel external balance is used for measuring lift, drag and pitching moment. Secondly, Tests are conducted on the aircraft model with and without winglet of two configurations at Reynolds numbers 1.7×10^5, 2.1×10^5, and 2.5×10^5 for different angle of attacks. Fuzzy logic approach is found as efficient for the representation, manipulation and utilization of aerodynamic characteristics. Therefore, the primary purpose of this work was to investigate the relationship between lift and drag coefficients, with free-stream velocities and angle of attacks, and to illustrate how fuzzy logic might play an important role in study of lift aerodynamic characteristics of an aircraft model with the addition of certain winglet configurations. Results of the developed fuzzy logic were compared with the experimental results. For lift coefficient analysis, the mean of actual and predicted values were 0.62 and 0.60 respectively. The coreelation between actual and predicted values (from FLS model) of lift coefficient in different angle of attack was found as 0.99. The mean relative error of actual and predicted valus was found as 5.18% for the velocity of 26.36 m/s which was found to be less than the acceptable limits (10%). The goodness of fit of prediction value was 0.95 which was close to 1.0.

***Keywords*—**Wind tunnel; Winglet; Lift coefficient; Fuzzy logic.

I. Introduction

THE present demand on fuel consumption has emphasized to improve aerodynamic efficiency of an aircraft through a wingtip device which diffuses the strong vortices produced at the tip and thereby optimise the span wise lift distribution, while maintaining the additional moments on the wing within certain limits. For this purpose one should be able to produce favorable effects of the flow field using wing tip and reducing the strength of the trailing vortex with the aid of wingtip devices.

The current study in winglets has been started for the last 25 years. Small and nearly vertical fins were installed on a KC-135A and flight was tested in 1979 and 1980 [1-2]. Whitcomb showed that winglets could increase an aircraft's range by as much as 7% at cruise speeds. A NASA contract [3] in the 1980s assessed winglets and other drag reduction devices, and they found that wingtip devices (winglet, feathers, sails, etc.) could improve drag due to lift efficiency by 10 to 15% if they are designed as an integral part of the wing. The "spiroid" wingtip [4] produces a reduction in induced drag at the same time blended winglet reduces drag. Flight tests on the Boeing Business Jet 737-400 resulted in a 7% drag reduction. Theoretical predictions had indicated that the configuration would have only a 1-2% improvement, and wind tunnel tests had shown only 2% drag reduction [5]. This indicates that wind tunnel test results of winglet configurations should be reviewed with some caution. The advantages of single winglets for small transports were investigated by Robert Jones [6], on which they can provide 10% reduction in induced drag compared with elliptical wings. Winglets are being incorporated into most new transports, including the Gulfstream III and IV business jets [7], the Boeing 747-400 and McDonnell Douglas MD-11 airliners, and the McDonnell Douglas C-17 military transport.

The first industry application of the winglet concept was in sailplane. The Pennsylvania State University (PSU) 94-097 airfoil had been designed for use on winglets of high-performance sailplanes [8]. To validate the design tools, as well as the design itself, the airfoil was tested in the Penn State Low-Speed, Low-Turbulence Wind Tunnel. Performance predictions from two well-known computer codes were compared to the data obtained experimentally, and both were found in good agreement with the wind tunnel measurements. Another investigation was carried out on wing tip airfoils by J. J. Spillman at the Cranfield Institute of technology in England [9]. He investigated the use of one to four sails on the wingtip fuel tank of a Paris MS 760 Trainer Aircraft. Experiments on flight test confirmed the wind tunnel tests and demonstrated shorter takeoff rolls and reduced fuel consumption [10]. Spillman later investigated wingtip vortex reduction due to wing tip sails, and found lower vortex energy 400-700 m behind the aircraft, although the rate of decay beyond that was

A. Hossain is with the Mechanical Engineering Department, International Islamic University Malaysia. He is also with the Mechanical Engineering Department, Universiti Industri Selangor (Tel: 603-3280-5122; Fax: 603-3280-6016; e-mail: altab75@unisel.edu.my).

A. Rahman is with the Mechanical Engineering Department, International Islamic University Malaysia (e-mail: arat@iiu.edu.my).

J. Hossen is with the Electrical Engineering Department, Multimedia University (e-mail: jakir.hossen@mmu.edu.my).

A. K.M.P. Iqbal is with the Mechanical Engineering Department, Universiti Industri Selangor (e-mail: parvez@unisel.edu.my).

SK. Hasan is with the Mechatronics Engineering Department, International Islamic University Malaysia (e-mail: shaon2k3@yahoo.com).

somewhat lower [11]. There has been limited investigation of multiple winglets for aircraft. The split-tip design [12] by Heinz Klug for an aircraft wing is considered a primitive multiple winglets which was created to exploit the non-planar wake geometry by reducing induced drag and wing stress. A biologist with an aerodynamic background has done extensive investigation of the split wingtips of soaring birds and he demonstrated that the tip slots of soaring birds reduce induced drag and increase the span factor of the wings [13]. He found remarkable improvements of slotted wingtips compared with conventional wing with a Clark Y airfoil by reducing the drag of 6%.

The multi-winglet [14] design was evaluated to demonstrate to improve the advanced performance potential over the baseline wing and an equivalent single winglet. The results of their wind tunnel testing show that certain multi-winglet configurations reduced the wing induced drag and improved L/D by 15-30% compared with the baseline 0012 wing. In Europe, an extension to the wing tip airfoils has been developed called Wing-Grid [15]. Wing-Grid is a set of multiple wing extensions added to the wing. These small wings are added at various angles so that their tip vortices do not interact to form a strong vortex. These smaller vortices dissipate the vortex energy so that the lift distribution is modified and the induced drag of the wing is reduced. But this concept is limited, since it is not able to change configuration in flight to optimise drag reduction. Aerodynamic characteristics for the aircraft model with and without winglet having NACA wing No. 65-3-218 has been explained [16]. An interaction matrix method has also been presented to revalidate the calibration matrix data provided by the manufacturer of the six-component external balance. The calibration of free stream velocity and flow quality in the test section has been established and documented [17-18].

Like many other real-world optimization, currently artificial intelligence methods have largely been used in the different areas including the aircraft industries. In the aircraft era, many expert systems were designed for predicting the aerodynamic characteristics of the aircraft. Based on the studies on characteristics of the aircraft, an intelligent system using Fuzzy Logic was introduced to predict the aerodynamic characteristics of the aircraft model. Fuzzy logic, an intelligent, knowledge based technique performs exceptionally well in non linear, complex systems [19-21]. This work presents the model of fuzzy system, comprising the control rules and term sets of variable with their relates fuzzy sets, enabling to express vague human concepts using fuzzy sets and also describe the corresponding inference systems based on fuzzy rules [22]. The aim of this study was the construction of fuzzy knowledge-based models for the prediction of aerodynamic characteristics of the aircraft model by controlling free stream velocities and angle of attack based on the Mamdani approach. A comparative performance analysis of this approach, by sampling data collected from the operation, was used to validate the fuzzy models.

II. Aircraft Modeling and Testing

A. Description of Model

The aircraft model used for the present study consists of a cylindrical body with NACA 65-3-218 airfoil rectangular wing. The aircraft model has a span of 0.66 m and a chord of 0.121 m. The elliptical shaped winglets (Fig. 1) were designed of wood with chord length of 0.121 m, which matches the chord length of the wing.

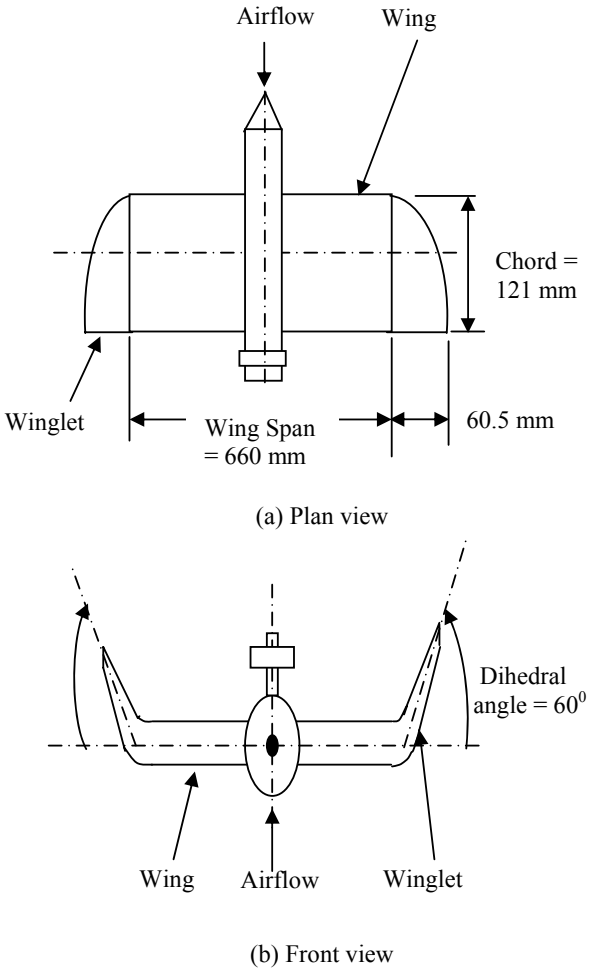

Fig.1. Schematic diagram of the aircraft model with winglet.

B. Theoretical Models

Coefficient of lift and coefficient of drag are defined as [23],

$$C_L = \frac{L}{\frac{1}{2}\rho_\infty {V_\infty}^2 S} \quad (1)$$

$$C_D = \frac{D}{\frac{1}{2}\rho_\infty {V_\infty}^2 S} \quad (2)$$

where L is the lift force in N, D is the drag force in N, ρ_∞ is the air density in kg/m^3, V_∞ is the free stream velocity in m/s, c is the chord length in m, and S is reference area in m^2.

Using equations of state for perfect gas the air density, ρ_∞ in kg/m^3 is defined as

$$\rho_\infty = \frac{p}{RT} \tag{3}$$

Where, p is the absolute pressure in N/m^2, T is the temperature in K, and R is the gas constant of air in Nm/(kg) (K).

Reynolds number based on the chord length is defined

$$\mathrm{Re} = \frac{\rho_\infty v_\infty c}{\mu_\infty} \tag{4}$$

Where, v_∞ is the free stream velocity in m/s; μ_∞ is the dynamic viscosity in kg/(m)(s) and c is the chord length in m.

The air viscosity, μ_∞ is determined using the Sutherland's equation [23] described below

$$\mu_\infty = 1.458\times10^{-6}\frac{T^{1.5}}{T+110.4} \tag{5}$$

Where, T is the temperature in K.

C. Experimental Procedure

Experiments were conducted in the Aerodynamics Laboratory Faculty of Engineering (University Putra Malaysia) with subsonic wind tunnel of 1 m ×1 m rectangular test section and 2.5 m long. The wind tunnel could be operated at a maximum air speed of 50 m/s and the turntable had a capacity for setting an angle of attack of 14 degree. The ambient pressure, temperature and humidity were recorded using barometer, thermometer, and hygrometer respectively for the evaluation of air density in the laboratory environment. Fig. 2 shows a photograph of the aircraft model with elliptical shaped winglet, which is mounted horizontally in the test section of the wind tunnel.

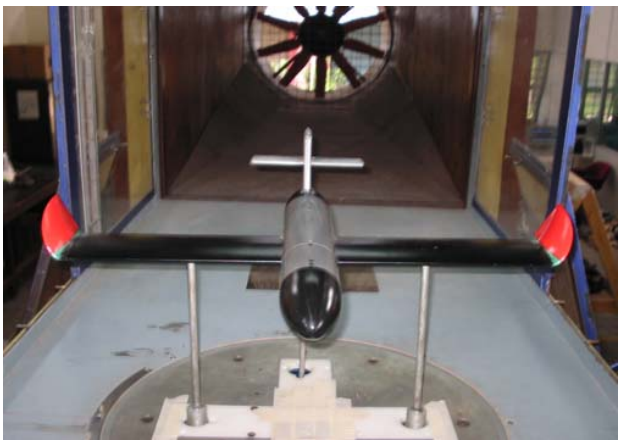

Fig.2. Aircraft Model with Elliptical shaped Winglet in test

The tests were carried out with free-stream velocity of 21.36 m/s, 26.76 m/s, and 32.15 m/s respectively with and without winglet of different configurations. The coefficient of lift (Table 1) and coefficient of drag (Table 2) were obtained from the experimental results as per the procedure explained in [16-17]. The simulations on the parameters were conducted by using the MATLAB.

TABLE I
LIFT COEFFICIENTS DATA

Winglet Configuration	Reynolds number 10^5	Lift coefficient, C_L		
		Initial angle of attack 0^0	Stall angle of attack 8^0	Final angle of attack 14^0
Without Winglet	1.7	0.237	0.805	0.657
	2.1	0.259	0.817	0.584
	2.5	0.306	0.879	0.733
Configuration 1 (0^0 angle)	1.7	0.299	0.829	0.641
	2.1	0.327	0.889	0.700
	2.5	0.359	0.934	0.713
Configuration 2 (60^0 angle)	1.7	0.386	0.930	0.729
	2.1	0.394	0.934	0.815
	2.5	0.416	1.018	0.885

TABLE II
DRAG COEFFICIENTS DATA

glet Configuration	Reynolds number 10^5	Drag coefficient, C_D		
		Initial angle of attack 0^0	Stall angle of attack 8^0	Final angle of attack 14^0
Without Winglet	1.7	0.085	0.104	0.249
	2.1	0.083	0.100	0.275
	2.5	0.065	0.085	0.211
Configuration 1 (0^0 angle)	1.7	0.053	0.058	0.136
	2.1	0.050	0.056	0.140
	2.5	0.049	0.053	0.128
Configuration 2 (60^0 angle)	1.7	0.070	0.078	0.166
	2.1	0.058	0.065	0.153
	2.5	0.047	0.060	0.134

D. Calibration of External Balance

Calibration of the six-component balance has been done to check the calibration matrix data provided by the manufacturer. Fig. 3 shows a photograph of the calibration rig used for the validation of calibration matrix, which is mounted on the upper platform of the balance in place of model. The relationship between signal readings, L_i and the loads, F_i applied on the calibration rig are given by the following matrix equation, the detailed procedure of calibration using Matlab software is explained elsewhere [17-18].

$$\{L_i\} = [K_{ij}]\{F_i\} \tag{6}$$

Where, $[K_{ij}]$ is the coefficient matrix, $\{L_i\}$ is the signal matrix, and $\{F_i\}$ is the load matrix.

Fig.3. Calibration rig mounted on the floor of the wind tunnel test section

The calibration matrix is obtained by finding the inverse of K_{ij}, coefficient matrix and it compares well with the calibration matrix data supplied by the manufacturer with six component external balance.

E. Speed Calibration

Subsonic wind tunnel of 2.5m length, 1m width and 1m height rectangular test section at the Aerodynamics Laboratory of the Aerospace Engineering Department, University Putra Malaysia was used for carrying out the experiments. The airflow velocity was controlled by the RPM controller of the wind tunnel. For the different Hz settings at the RPM controller the flow velocities in wind tunnel test section were recorded using six-component external balance software. In addition to this dynamic pressure at the pitot tube was recorded with digital manometer and corresponding velocities were calculated [16, 24]. The validity of the digital manometer was confirmed by comparing the dynamic pressure measured through the digital manometer and through the tube manometer used along with the pitot tube mounted in the test section. The flow velocity versus RPM controller speed curves was plotted for the data obtained through six components external balance software, digital manometer and tube manometer and were given in Fig. 4. Least square fit lines were drawn through the data and the corresponding lines were given in Fig.4. It was observed that the curves for the digital manometer and the tube manometer readings were practically the same whereas the curve for the data using six component external balance software deviated a little from the other two curves. The experimental error using the external balance was nearly 6%. The flow velocity readings of the external balance are corrected through the following calibration equation obtained through the data shown in Fig.5,

$$y = 1.0796x - 0.2336 \quad (7)$$

Where x denotes external balance software velocity (m/s) and y denotes digital manometer velocity (m/s).

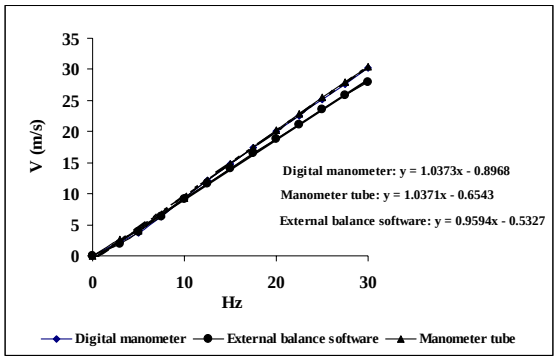

Fig.4. Free stream velocity vs. RPM controller speed.

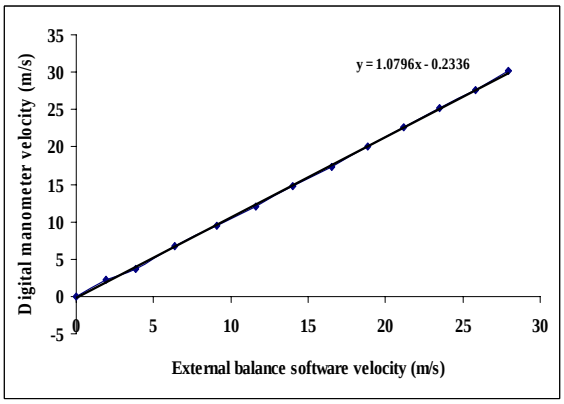

Fig.5. Flow velocity calibration for external balance

Using the equation (7), the actual value of free stream air velocity would be 21.36 m/s for corresponding 20 m/s of air velocity from six-component external balance software.

F. Flow Uniformity

The dynamic pressure was measured using digital manometer at different locations in the test section in YZ-plane by means of a pitot tube for a RPM controller setting of 15 Hz. For different locations of the measurement grid the experiments were repeated three times and the experimental data was given in [16]. The average (mean) dynamic pressure was obtained from the measured dynamic pressure data. The dynamic pressure variations from the mean were calculated in percentage at different locations of YZ-plane. Using these data dynamic pressure variations from the mean (%) versus distance from wind tunnel floor (cm) were plotted as shown in Fig.6. It was observed that the variation of dynamic pressure in the test section was within ± 0.5% which indicated that the there was very good uniformity of flow in the test section of the wind tunnel during the experimental set up for the aircraft model with and without winglet.

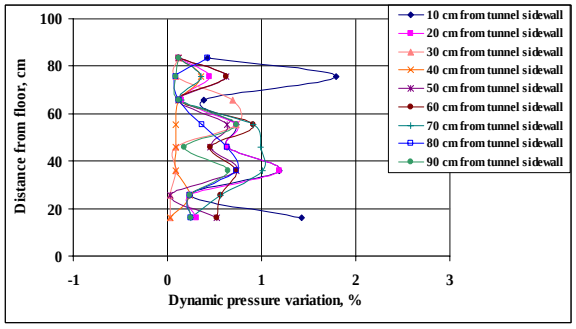

Fig.6. Dynamic pressure variation in the test section.

III. Fuzzy Logic

Fuzzy Logic approach was introduced in this work for the prediction of aerodynamic characteristics of the aircraft model with and without winglet. The main advantage of Fuzzy Logic is that it can be tuned and adapted if necessary, thus enhancing the degree of freedom of the system [25]. For implementation of fuzzy values into the of aircraft model by using Fuzzy logic system (FLS), free stream velocity (FV) and angle of attack (AA) were used as input parameters and lift coefficient (C_L) and drag coefficient (C_D) were used as output. For fuzzification of these factors the linguistic variables very low (VL), low (L), medium (M), high (H), and very high (VH) were used for the inputs and output. In this study, the center of gravity (Centroid) method for defuzzification was used because these operators assure a linear interpolation of the output between the rules. The units of the used factors were: FV (m/s), AA (degree), and C_L and C_D are dimensionless. With the fuzzy sets defined, it is possible to associate the fuzzy sets in the form of fuzzy rules. For the two inputs and two outputs, a fuzzy associated memory or decision (also called rule) table is developed as shown in Table 3. Total of 25 rules were formed.

Using MATLAB FUZZY Toolbox, prototype triangular fuzzy sets for the fuzzy variables, namely, free stream velocity (FV), angle of attack (AA), coefficient of lift (C_L) and coefficient of drag (C_D) were set up. The term of parameters (membership functions) are presented in the Fig. 7 (a), (b), (c) and (d).

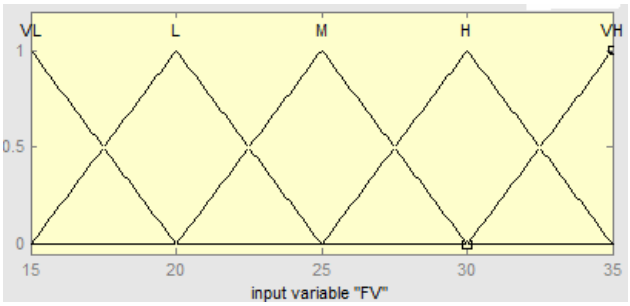

Fig.7a. Prototype membership functions for free stream velocity (FV).

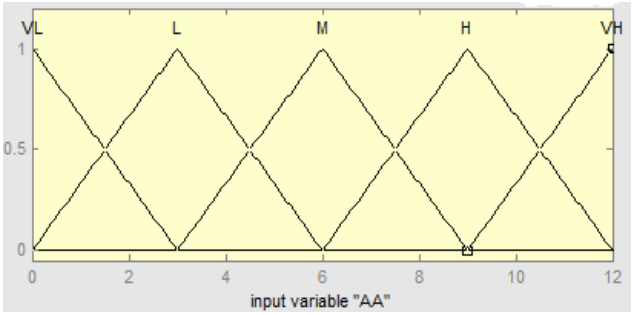

Fig.7b. Prototype membership functions for angle of attack (AA).

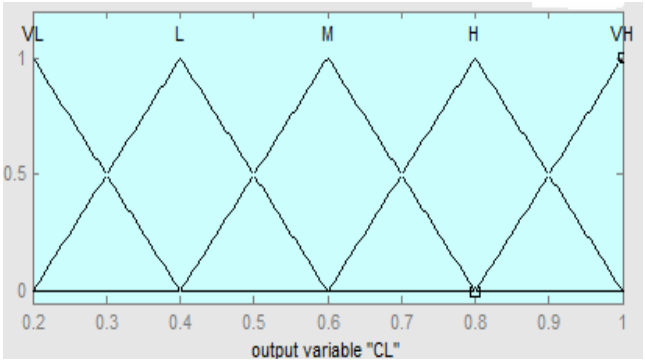

Fig.7c. Prototype membership functions for coefficient of lift (C_L).

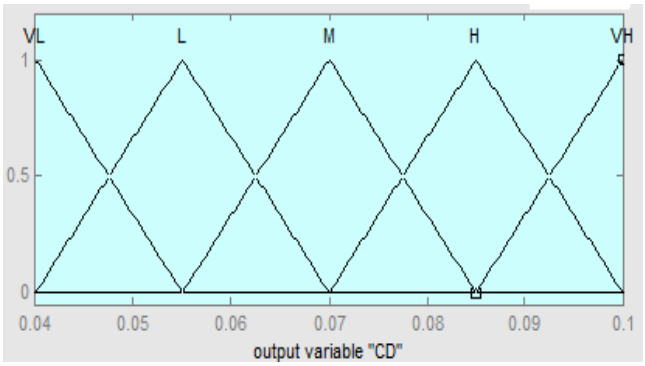

Fig.7d. Prototype membership functions for coefficient of drag (C_D).

The membership values used for the FLS were obtained from the formulas presented analytically below. These membership functions helped in converting numeric variables into linguistic terms. There is a degree of membership for each linguistic term that applies to that input variable. These formulas were determined by using measurement values. The linguistic expressions and membership functions for inputs and output were obtained from the developed rules and following formula.

$$\mu_{FV}(i_1)=\left\{\begin{array}{l}\mu_{VL}(i_1)=\dfrac{20-i_1}{5};15\le i_1\le 20\\ \mu_{L}(i_1)=\left\{\begin{array}{l}\dfrac{i_1-15}{5};15\le i_1\le 20\\ \dfrac{25-i_1}{5};20\le i_1\le 25\end{array}\right\}\\ \mu_{M}(i_1)=\left\{\begin{array}{l}\dfrac{i_1-20}{5};20\le i_1\le 25\\ \dfrac{30-i_1}{5};25\le i_1\le 30\end{array}\right\}\\ \mu_{H}(i_1)=\left\{\begin{array}{l}\dfrac{i_1-25}{5};25\le i_1\le 30\\ \dfrac{35-i_1}{5};30\le i_1\le 35\end{array}\right\}\\ \mu_{VH}(i_1)=\dfrac{i_1-30}{5};30\le i_1\le 35\end{array}\right\} \quad (8)$$

$$\mu_{AA}(i_2)=\left\{\begin{array}{l}\mu_{VL}(i_2)=\dfrac{3-i_2}{3};0\le i_2\le 3\\ \mu_{L}(i_2)=\left\{\begin{array}{l}\dfrac{i_2}{3};0\le i_2\le 3\\ \dfrac{6-i_2}{3};3\le i_2\le 6\end{array}\right\}\\ \mu_{M}(i_2)=\left\{\begin{array}{l}\dfrac{i_2-3}{3};3\le i_2\le 6\\ \dfrac{9-i_2}{3};6\le i_2\le 9\end{array}\right\}\\ \mu_{H}(i_2)=\left\{\begin{array}{l}\dfrac{i_2-6}{3};6\le i_2\le 9\\ \dfrac{12-i_2}{3};9\le i_2\le 12\end{array}\right\}\\ \mu_{VH}(i_2)=\dfrac{i_2-9}{3};9\le i_2\le 12\end{array}\right\} \quad (9)$$

$$\mu_{CL}(o_1)=\left\{\begin{array}{l}\mu_{VL}(o_1)=\dfrac{0.4-o_1}{0.2};0.2\le o_1\le 0.4\\ \mu_{L}(o_1)=\left\{\begin{array}{l}\dfrac{o_1-0.2}{0.2};0.2\le o_1\le 0.4\\ \dfrac{0.6-o_1}{0.2};0.4\le o_1\le 0.6\end{array}\right\}\\ \mu_{M}(o_1)=\left\{\begin{array}{l}\dfrac{o_1-0.4}{0.2};0.4\le o_1\le 0.6\\ \dfrac{0.8-o_1}{0.2};0.6\le o_1\le 0.8\end{array}\right\}\\ \mu_{H}(o_1)=\left\{\begin{array}{l}\dfrac{o_1-0.6}{0.2};0.6\le o_1\le 0.8\\ \dfrac{1-o_1}{0.2};0.8\le o_1\le 1.0\end{array}\right\}\\ \mu_{VH}(o_1)=\dfrac{o_1-0.8}{0.2};0.8\le o_1\le 1.0\end{array}\right\} \quad (10)$$

$$\mu_{CD}(o_2)=\left\{\begin{array}{l}\mu_{VL}(o_2)=\dfrac{0.055-o_2}{0.015};0.04\le o_2\le 0.055\\ \mu_{L}(o_2)=\left\{\begin{array}{l}\dfrac{o_2-0.055}{0.015};0.04\le o_2\le 0.055\\ \dfrac{0.07-o_2}{0.015};0.055\le o_2\le 0.07\end{array}\right\}\\ \mu_{M}(o_2)=\left\{\begin{array}{l}\dfrac{o_2-0.055}{0.015};0.055\le o_2\le 0.07\\ \dfrac{0.085-o_2}{0.015};0.07\le o_2\le 0.085\end{array}\right\}\\ \mu_{H}(o_2)=\left\{\begin{array}{l}\dfrac{o_2-0.07}{0.015};0.07\le o_2\le 0.085\\ \dfrac{0.1-o_2}{0.015};0.085\le o_2\le 0.1\end{array}\right\}\\ \mu_{VH}(o_2)=\dfrac{o_2-0.085}{0.015};0.085\le o_2\le 0.1\end{array}\right\} \quad (11)$$

In defuzzification stage, truth degrees (μ) of the rules were determined for the each rule by aid of the min and then by taking max between working rules. For example, for FV = 27 m/s and AA = 8^0, the rules 13, 14, 18 and 19 will be fired. To get the fuzzy inputs the values for FV and AA are substituted into Eq. (8), and (9) and values are obtained as

$\mu_M(FV)=0.6,\ \mu_H(FV)=0.4,$

$\mu_M(AA)=0.33,\ \mu_H(AA)=0.67$

The strength (truth values) of the four rules are obtained as

$$\alpha_{13}=\min\{\mu_M(FV),\mu_M(Aa)\}=\min(0.6,0.33)=0.33$$

$$\alpha_{14}=\min\{\mu_M(FV),\mu_H(AA)\}=\min(0.6,0.67)=0.6$$

$$\alpha_{18}=\min\{\mu_H(FV),\mu_M(AA)\}=\min(0.4,0.33)=0.33$$

$$\alpha_{19}=\min\{\mu_H(FV),\mu_H(AA)\}=\min(0.4,0.67)=0.4$$

For rule (13) the consequent is "coefficient of lift (C_L) and coefficient of drag (C_D) are medium". The membership function for the conclusion reached by rule (13), which is denoted as μ_{13}, is given by

$\alpha_{13}(CL)=\min\{0.33,\mu_M(CL)\},\alpha_{13}(CD)=\min\{0.33,\mu_M(CD)\}$

Similarly, the membership functions for the conclusion reached by rule (14), (18) and (19), are

$\alpha_{14}(CL)=\min\{0.6,\mu_H(CL)\},\ \alpha_{14}(CD)=\min\{0.6,\mu_H(CD)\}$

$\alpha_{18}(CL)=\min\{0.33,\mu_M(CL)\},\alpha_{18}(CD)=\min\{0.33,\mu_M(CD)\}$

$\alpha_{19}(CL)=\min\{0.4,\mu_H(CL)\},\alpha_{19}(CD)=\min\{0.4,\mu_H(CD)\}$

The output denoted by "$CL^{\ crisp}$" and "$CD^{\ crisp}$" can be calculated that best represents the conclusions of the fuzzy controller that are represented with the implied fuzzy sets. Due to its popularity, the "center of gravity" (COG) defuzzification method is used for combing the recommendations represented by the implied fuzzy sets from all the rules [22].

The output membership values are multiplied by their corresponding singleton values and then are divided by the sum of membership values.

$$CL^{crisp}=CD^{crisp}=\frac{\sum b_i\mu_i}{\sum\mu_i} \quad (12)$$

Where b_i is the position of the singleton in i the universe, and $\mu_{(i)}$ is equal to the firing strength of truth values of rule i.

Using the above mentioned rules in Fig. 7(c), and 7(d), the following values are obtained as

For CL^{crisp}, $b_{13} = 0.6$, $b_{14} = 0.8$, $b_{18} = 0.6$, $b_{19} = 0.8$

For CD^{crisp}, $b_{13} = 0.07$, $b_{14} = 0.085$, $b_1 = 0.07$, $b_{19} = 0.085$

The coefficient of lift, and coefficient of drag were obtained using equation (12) with membership values from the rules as 0.72, and 0.08 respectively.

In addition, the predictive ability of developed system was investigated according to mathematical and statistical methods. In order to determine the relative error (ε) of system, the following equation was used:

$$\varepsilon = \sum_{i=1}^{n} \left| \frac{y - \hat{y}}{y} \right| \frac{100\%}{n} \tag{13}$$

Where n is the number of observations, y is the actual value, and $\hat{y}$ is the predicted value. The relative error gives the deviation between the predicted and experimental values and it is required to reach zero. In addition, goodness of fit (η) of predicted system was calculated by following equation:

$$\eta = \sqrt{1 - \frac{\sum_{i=1}^{n} \left(y - \hat{y} \right)^2}{\sum_{i=1}^{n} \left(y - \bar{y} \right)^2}} \tag{14}$$

Where $\bar{y}$ is the mean of actual values. The goodness of fit also gives the ability of the developed system and its highest value is 1.

IV. Results And Discussions

A. Test Conditions

The aircraft model tests with different configuration of winglets and without winglet were carried out at Reynolds numbers 1.7×10^5, 2.1×10^5, and 2.5×10^5. The measured values for the lift force, and drag force for the various configurations were given in Ref. [16-17] and coefficient of lift and coefficient of drag were calculated as per the procedures explained.

B. Coefficient of Lift

The lift coefficient characteristics of the aircraft model without winglet under test have been shown in Fig. 8 for all Reynolds numbers. The lift increases with increase in angle of attack to a maximum value and thereby decreases with further increase in angle of attack. At the maximum value of the angle of attack the lift coefficient characteristic has a mixed behavior. At the maximum angle of attack of 14 degree the lift coefficients are 0.657, 0.584, and 0.733 respectively for the Reynolds numbers of 1.7×10^5, 2.1×10^5, and 2.5×10^5. The reason for a drop in lift coefficient beyond a certain angle of attack e.g. 8^0 is probably due to the flow separation, which occurs over the wing surface instead of having a streamlined laminar flow there. This condition is called stalling condition and stalling angle happens to be approximately 8^0 for all the Reynolds numbers under the present study.

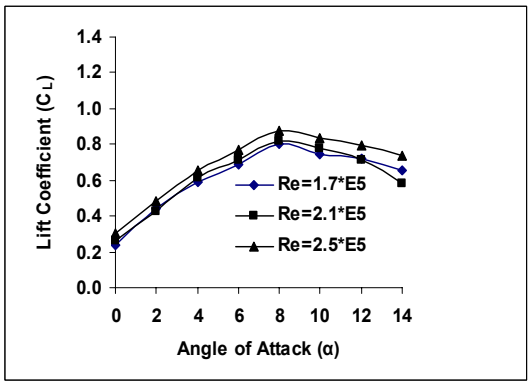

Fig.8. Lift Coefficients for the Aircraft Model without Winglet.

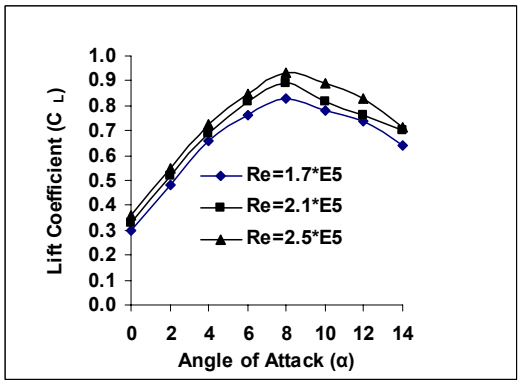

Fig.9. Lift Coefficients for the Aircraft Model with Elliptical Winglet at 0^0 (Configuration 1).

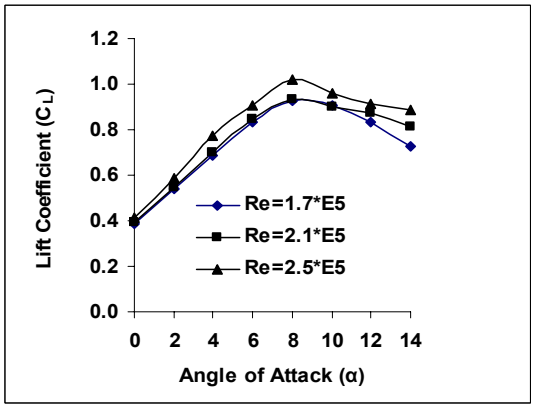

Fig.10. Lift Coefficients for the Aircraft Model with Elliptical Winglet at 60^0 (Configuration 2).

The lift coefficient data for elliptical winglet for the two configurations i.e. configuration 1 (winglet inclination 0^0), and configuration 2 (winglet inclination 60^0) is given in Fig. 9 and 10 respectively. In case of the winglet for both configurations 1 and 2 a similar pattern is observed. For the maximum Reynolds number of $2.5x10^5$ the lift coefficients for configuration-1 (Fig. 9) and for configuration-2 (Fig. 10) are

0.934 and 1.018 respectively corresponding to an angle of attack of 8^0 which is stall angle of attack also.

The drag coefficients of the aircraft model under test for all Reynolds numbers are shown in Fig. 11. The drag increases slowly with increase in angle of attack to a certain value and then it increases rapidly with further increase in angle of attack. The value of the drag coefficient appears to decrease with the increase in Reynolds number. At the maximum angle of attack of 14 degree the drag coefficients are 0.249, 0.275, and 0.211 respectively for the Reynolds numbers of 1.7×10^5, 2.1×10^5, and 2.5×10^5. The rapid increase in drag coefficient, which occurs at higher values of angle of attack, is probably due to the increasing region of separated flow over the wing surface, which creates a large pressure drag.

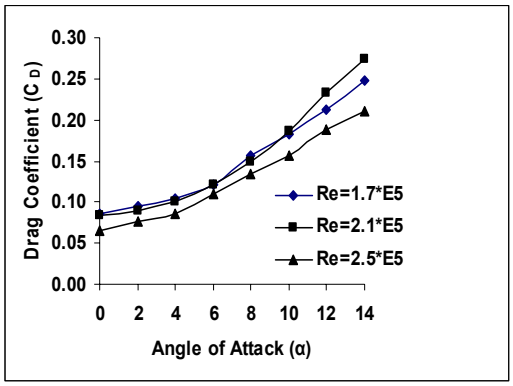

Fig.11. Drag Coefficients for the Aircraft model without Winglet.

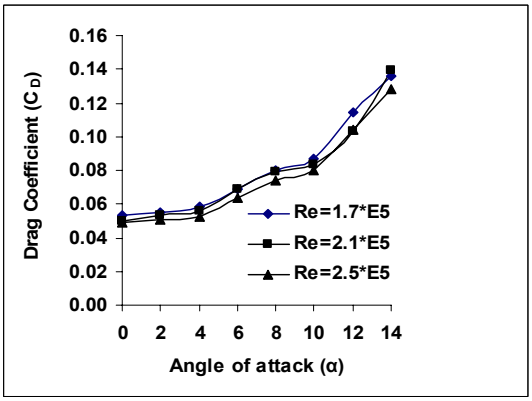

Fig.12. Drag Coefficients for the Aircraft model with Elliptical winglet 0^0 (Configuration 1).

The drag coefficient data for elliptical winglet for the two configurations i.e. configuration 1 (winglet inclination 0^0), and configuration 2 (winglet inclination 60^0) is given in Figure 12 and 13. In case of elliptical winglet for both configurations 1 and 2 a similar pattern has been observed. In general it is observed that the coefficient of drag decreases with the increase of Reynolds number. For maximum Reynolds number of 2.5×10^5 and at 0^0angle of attack the drag coefficients for the elliptical winglet of configuration-1 (Fig. 12) and elliptical winglet of configuration-2 (Fig. 13) are 0.049 and 0.047 respectively.

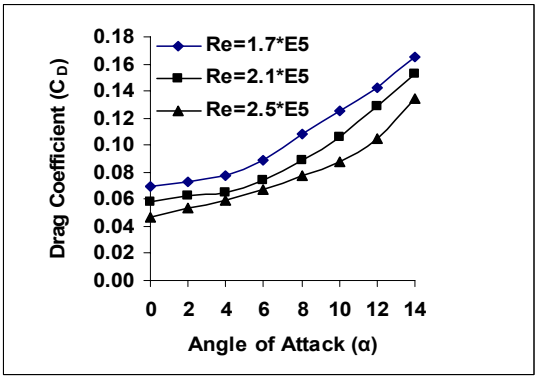

Fig.13: Drag Coefficients for the Aircraft model with Elliptical Winglet 60^0 (Configuration 2)

The results of the developed fuzzy logic system (FLS) were compared with the experimental results. For lift coefficient analysis, the mean of actual and predicted values were 0.62 and 0.60 respectively. The coreelation between actual and predicted values (from FLS model) of lift coefficient in different angle of attack was given in Fig. 14. The relationship was significant for all parameters. The correlation coefficient of reltionship was found as 0.99. The mean relative error of actual and predicted valus (from FLS model) was found as 5.18% for the velocity of 26.36 m/s which was found to be less than the acceptable limits (10%). The goodness of fit of prediction (from FLS model) value was found as 0.95 which was found to be close to 1.0. The above indices indicate that the system is qualified to replace the work of an operator.

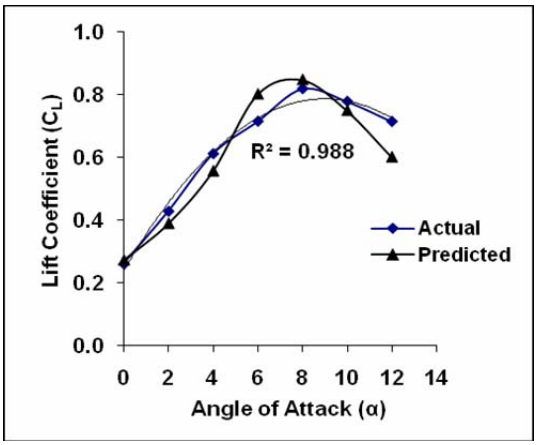

Fig. 14. Correlation between actual and predicted values of lift coefficient.

V. Conclusion

This paper presents an adaptive approach based on the use of fuzzy logic for the prediction of lift coefficient for the aircraft model. In comparison to other predictive modeling

techniques, fuzzy models have the advantage of being simple (rule base and membership functions) and robust. In this study, according to evaluation criteria of predicted performances of developed fuzzy knowledge-based model was found to be valid. However, the conclusions drawn from this investigation are as follows:

(a) Elliptical winglet at 60 degree incidence improves the lift curve slope and produces more lift than the aircraft model without winglet.
(b) Elliptical winglet improves the lift by drag ratio and thus reduces the drag.
(c) The developed model can be used as a reference for the prototype.
(d) This investigation provides a better understanding for the winglet concept and its inclusion to the wing of aircraft model**.**

ACKNOWLEDGMENT

The authors are grateful for the support provided by financial assistance from the University Putra Malaysia (UPM) for the overall facilities.

REFERENCES

[1] R.T.Whitcomb, A Design Approach and Selected Wind-Tunnel Results at High Subsonic Speeds for Wing-Tip Mounted Winglets, *NASA TN D*-8260, 1976.
[2] R. T. Whitcomb, Methods for Reducing Aerodynamic Drag, *NASA* Conference Publication 2211, Proceedings of Dryden Symposium, Edwards, California, 1981.
[3] J. E.Yates, and C. Donaldson, Fundamental Study of Drag and an Assessment of Conventional Drag-Due-To-Lift Reduction Devices, *NASA* Contract Rep 4004, 1986.
[4] B. Louis, Gratzer, Spiroid-Tipped Wing. *U. S. patent* 5, 102,068, 1992.
[5] V. F. Reginald, Vortex Reducing Wing Tip, *U. S. Patent* 4, 108, 403, 1978.
[6] R. T. Jones, Improving the Efficiency of Smaller Transport Aircraft, 14th *Congress of the International Council of the Aeronautical Sciences*, proceeding, Vol. 1, Toulouse, Fr. 1984.
[7] Chandrasekharan, M. Reuben, Murphy, R. William, Taverna, P. Frank, and B. W. Charles, Computational Aerodynamic Design of the Gulftream IV Wing, *AIAA-85-0427,* 1985..
[8] M. D. Maughmer, S. S. Tmothy, and S. M. Willits, The Design and Testing of a Winglet Airfoil for Low-Speed Aircraft, *AIAA* Paper 2001-2478, 2001.
[9] J. J. Spillman, The use of wing tip sails to reduce vortex drag, *Aeronautical Journal*, September, pp. 387-395, 1978.
[10] J. J. Spillman, H. Y. Ratcliffe, and A. McVitie, Flight experiments to evaluate the effect of wing-tip sails on fuel consumption and handling characteristics, *Aeronautical Journal*, July, pp. 279-281, 1979.
[11] J. J. Spillman, and M. J. Fell, The effects of wing tip devices on (a) the performance of the Bae Jetstream (b) the far-field wake of a Paris Aircraft, *Paper 31A, AGARD CP No. 342, Aerodynamics of Vortical Type Flows in Three Dimensions,* April, pp. 31A-1-11, 1983.
[12] H. G. Klug, Auxiliary Wing Tips for an Aircraft, *U. S. Patent* 4722499, 1988.
[13] A.T. Vance, Gliding Birds: Reduction of Induced Drag by Wing Tip Slots between the Primary Feathers, *Journal of Experimental Biology*, Vol. 180 (1), pp. 285-310, 1993.
[14] M. J. Smith, N. Komerath, R. Ames, O. Wong, and J. Pearson, Performance Analysis of a Wing with Multiple Winglets, *AIAA* Paper-2001-2407, 2001.
[15] L. U. Roche, and S. Palffy, WING-GRID, a Novel Device for Reduction of Induced Drag on Wings, Proceedings of ICAS 96, Sorrento, September, 1996.
[16] A. Hossain, P. R. Arora, A. Rahman, A. A. Jaafar, and A. K. M. P. Iqbal, Analysis of Aerodynamic Characteristics of an Aircraft Model with and Without Winglet, *Jordan Journal of Mechanical and Industrial Engineering*. Vol. 2, No. 3, pp. 143-150, 2008.
[17] R. A. Prithvi, A. Hossain, A. A. Jaafar, P. Edi, T. S. Younis, and M. Saleem, Drag Reduction in Aircraft Model using Elliptical Winglet, *Journal - The Institution of Engineers, Malaysia (IEM)*, Vol. 66, No. 4, pp. 1-8, 2005.
[18] P. R. Arora, A. Hossain, P. Edi, A. A. Jaafar, T.S. Younis, and M. Saleem, Six-Component External Balance: A Calibration Study, Proceedings of AEROTECH-2005, Putra Jaya, Malaysia.
[19] A. Hossain, R. Ataur, M. Rahman, SK. Hasan, and H. Jakir, Prediction of Power Generation of Small Scale Vertical Axis Wind Turbine Using Fuzzy Logic, *Journal of Urban and Environmental Engineering (JUEE*), Vol. 3, No.2, pp. 43-51, 2009.
[20] A. Al-Anbuky, S. Bataineh, and S. Al-Aqtash, Power demand prediction using fuzzy logic, *Control Engineering Practice*, Vol. 3, No. 9, pp. 1291-1298, 1995.
[21] K. Carman, Prediction of soil compaction under pneumatic tires a using fuzzy logic approach, *Journal of Terramechanics*, Vol.45, pp.103-108, 2008.
[22] K.M. Passino, and S. Yurkovich, Fuzzy control, Addison Wesley Longman, Inc. Menlo park, CA, USA, 1998.
[23] J. J. Bertin, *Aerodynamics for Engineers*. New Jersey, Prentice-Hall, Inc. 2002.
[24] A. Hossain, P. R. Arora, A. Rahman, A. A. Jaafar, A.K.M.P. Iqbal, and M. Ariffin, Lift Analysis of an Aircraft Model with and without Winglet, 7th International Conference on Mechanical Engineering, ICME 2007, 28-30 December, 2007, Dhaka, Bangladesh.
[25] A. Rajagopalan, G. Washington, G. Rizzani, and Y. Guezennec, Development of Fuzzy Logic and Neural Network Control and Advanced Emissions Modeling for Parallel Hybrid Vehicles, *Center for Automotive Research, Intelligent Structures and Systems Laboratory,* Ohio State University, USA, December 2003.